



Research article

Synchronization control of time-delay neural networks via event-triggered non-fragile cost-guaranteed control

Wenjing Wang¹, Jingjing Dong¹, Dong Xu¹, Zhilian Yan^{2,*} and Jianping Zhou¹

¹ School of Computer Science & Technology, Anhui University of Technology, Ma'anshan 243032, China

² School of Electrical & Information Engineering, Anhui University of Technology, Ma'anshan 243032, China

* **Correspondence:** Email: zhilian_yan@163.com.

Abstract: This paper is devoted to event-triggered non-fragile cost-guaranteed synchronization control for time-delay neural networks. The switched event-triggered mechanism, which combines periodic sampling and continuous event triggering, is used in the feedback channel. A piecewise functional is first applied to fully utilize the information of the state and activation function. By employing the functional, various integral inequalities, and the free-weight matrix technique, a sufficient condition is established for exponential synchronization and cost-related performance. Then, a joint design of the needed non-fragile feedback gain and trigger matrix is derived by decoupling several nonlinear coupling terms. On the foundation of the joint design, an optimization scheme is given to acquire the minimum cost value while ensuring exponential stability of the synchronization-error system. Finally, a numerical example is used to illustrate the applicability of the present design scheme.

Keywords: neural networks; cost-guaranteed control; time delay; event-triggered control; synchronization

1. Introduction

Neural networks (NNs) are a kind of intricate nonlinear information processing systems with functional features such as self-learning, self-organizing, noise-resistance and distortion resistance, and thus can be utilized to solve problems that are difficult to handle by using traditional information processing approaches. Not surprisingly, NNs have been successfully applied across a variety of fields including speech synthesis [1], grammar learning [2], pattern classification [3] and time series prediction [4]. It is well known that time delays are almost unavoidable in the circuit implementation

of NNs, and that are capable of causing oscillation of the NNs and even generating more complicated chaotic attractors. In view of this, the study of time-delay NNs (TDNNs) has drawn a great deal of attention from the academic communities of automation, mathematics and physics [5–13]. Particularly, chaos synchronization of TDNNs has become one of the research hotspots due to its importance in nonlinear theory and strong application potential in many fields, including parameter identification, image encryption and secure communication [14–16]. The objective of chaos synchronization is to ensure that the state trajectories of the drive and response system tend to be consistent [17]. In order to achieve this objective, various control methodologies, including nonlinear feedback control [18], observer-based control [19], adaptive control [20] and sampled-data control [21, 22], have been proposed in the literature.

In the automation community, event-triggered control (ETC) has been increasingly recognized as an ideal control strategy as it can not only ensure the desired control performance but it can also mitigate the over-occupancy of communication channels in digital communication networks [23–26]. Within such a control strategy, the measurement signal is transmitted to the input of the controller only when pre-specified events occur. In this way, ETC can successfully reduce the update frequency of the controller, thereby saving computational and network resources. At present, there are several meaningful ETC mechanisms that have been put forward, including the continuous ETC mechanism [27], discrete ETC mechanism [28], self-triggered ETC mechanism [29], dynamic ETC mechanism [30], switched event-triggered control (SETC) mechanism [31] and so on. As shown in [31–35], the SETC mechanism ensures a positive minimum inter-event interval between any two adjacent events, thus avoiding the so-called Zeno phenomenon. In addition, it can markedly reduce the data transmission frequency while maintaining performance.

Very recently, the chaos synchronization of TDNNs based on the SETC mechanism has been investigated by many researchers, and a few meaningful results have been proposed [36–38]. An implicit assumption in these reports is that there are no uncertainties of the controller gain. However, fluctuations of control gains may occur inevitably owing to component aging, round-off errors in calculations, and conversion between digital and analog [39–42]. Such fluctuations can result in performance degradation or even instability of the closed-loop system [43]. In addition, the control cost has not been considered in the above literature. However, while achieving the purpose of control, there may be certain requirements for the cost to be paid. Based on the above discussion, the non-fragile cost-guaranteed synchronization control (CGSC) for TDNNs under the SETC mechanism is a significant issue that deserves thorough investigation. However, to our knowledge, there are no relevant results so far and the topic remains open and challenging.

Motivated by the above observations, the study was designed to explore the SETC mechanism-based non-fragile CGSC for TDNNs. The following are the main contributions of our work:

- 1) A piecewise functional was developed by fully utilizing the information of the state and activation function of the switched synchronization-error system;
- 2) A joint design of the needed non-fragile feedback gain and trigger matrix has been derived by eliminating nonlinear coupling terms;
- 3) An optimization method was developed to acquire the minimum cost value while ensuring exponential stability by using the properties of matrix trace operations.

The rest of this paper is organized as follows. The models of drive and response TDNNs and some necessary preliminaries are provided in Section 2. In Section 3, the non-fragile exponential

synchronization and cost-related performance analysis under the SETC mechanism is discussed and the results of the joint design and its optimization are presented. In Section 4, a numerical simulation is described to verify the validity of the developed results. In the last section, we give the conclusion.

Notations: $\mathbb{R}^{l \times n}$ represents $l \times n$ -dimensional real matrices, \mathbb{R}^l stands for the l -dimensional Euclidean space and $\|\cdot\|$ represents the corresponding vector norm. For a square matrix W , $W > 0$ means that W is positive semi-definite; I and 0 represent the identity matrix and the zero matrix with the proper dimensions, respectively; $\lambda_{\min}(W)$ is used to represent the smallest eigenvalue of W . Furthermore, we use $*$ to denote a symmetry term in a matrix, and we denote a diagonal matrix by $\text{diag}\{\cdot\}$.

2. Preliminaries

Consider a TDNN described by:

$$\dot{x}(t) = -\mathcal{A}x(t) + \mathcal{B}f(x(t)) + \mathcal{B}_\tau f(x(t - \tau(t))) + I, \quad (2.1a)$$

$$y(t) = Cx(t), \quad (2.1b)$$

in which $x(t) = [x_1(t), \dots, x_p(t)]^T \in \mathbb{R}^p$ denotes the neuron state, $y(t) = [y_1(t), \dots, y_q(t)]^T \in \mathbb{R}^q$ represents the output vector, $\mathcal{A} \in \mathbb{R}^{p \times p}$ stands for the self-feedback matrix, $\mathcal{B} \in \mathbb{R}^{p \times p}$ and $\mathcal{B}_\tau \in \mathbb{R}^{p \times p}$ are the connection weight matrices, $C \in \mathbb{R}^{q \times p}$ is a constant real matrix, $I \in \mathbb{R}^p$ represents a constant input and $\tau(t)$ refers to the time-varying delays satisfying $0 \leq \tau(t) \leq \tau$ and $\dot{\tau}(t) \leq \mu < 1$. $f(x(t)) = [f_1(t), \dots, f_p(t)]^T \in \mathbb{R}^p$ denotes the neuron activation function, satisfying the following hypothesis:

Assumption 1. For any $s_1, s_2 \in \mathbb{R}, s_1 \neq s_2$, there exists a positive matrix $L = \text{diag}\{L_1, \dots, L_p\}$ such that

$$0 \leq \frac{f_i(s_2) - f_i(s_1)}{s_2 - s_1} \leq L_i, i = 1, \dots, p. \quad (2.2)$$

Remark 1. A number of assumptions about the activation function have been proposed over the last several decades. Among these, Assumption 1 has been widely used in existing studies [22, 44, 45]. Many common functions satisfy such an assumption, such as the sigmoid function $g(s) = (1 + e^{-s})^{-1}$, the piecewise linear function $g(s) = 0.5(|s + 1| - |s - 1|)$, and tanh function $g(s) = \tanh(s)$.

Remark 2. The TDNN in (2.1) covers many famous NN models, such as cellular NNs, BAM NNs and Hopfield NNs, as special cases. In addition, as shown in [46], the network model is capable of generating complex chaotic attractors, thus affording it with strong application potential in secure communication and image encryption.

TDNN (2.1) is considered a drive system. We set the response system as

$$\hat{x}(t) = -\mathcal{A}\hat{x}(t) + \mathcal{B}f(\hat{x}(t)) + \mathcal{B}_\tau f(\hat{x}(t - \tau(t))) + u(t) + I, \quad (2.3a)$$

$$\hat{y}(t) = C\hat{x}(t), \quad (2.3b)$$

in which $\hat{x}(t) = [\hat{x}_1(t), \dots, \hat{x}_p(t)]^T \in \mathbb{R}^p$ and $\hat{y}(t) = [\hat{y}_1(t), \dots, \hat{y}_q(t)]^T \in \mathbb{R}^q$ are the state and the output of the response system, respectively. $u(t) \in \mathbb{R}^p$ denotes the system control input, which has the form

$$u(t) = -\bar{\mathcal{K}}(\hat{y}(t) - y(t)),$$

where $\bar{\mathcal{K}} = \mathcal{K} + \Delta\mathcal{K}$. $\mathcal{K} \in \mathbb{R}^{p \times q}$ refers to the non-fragile controller gain to be designed and $\Delta\mathcal{K}$ denotes the possible gain perturbation which is assumed to be of the form

$$\Delta\mathcal{K} = \mathcal{G}\mathcal{T}(t)\mathcal{M}, \quad (2.4)$$

where \mathcal{G} and \mathcal{M} are known constant matrices and $\mathcal{T}(t)$ is an uncertain parameter matrix satisfying $\mathcal{T}^T(t)\mathcal{T}(t) \leq I$. Here, the gain perturbation is assumed to have the additive norm-bounded nonlinearity form. For multiplicative norm-bounded nonlinearity, one may refer to [11].

Then, by defining synchronization errors $\varepsilon(t) = \hat{x}(t) - x(t)$ and $\bar{y}(t) = \hat{y}(t) - y(t)$, we can establish the error system as follows:

$$\dot{\varepsilon}(t) = -\mathcal{A}\varepsilon(t) + \mathcal{B}\bar{f}(\varepsilon(t)) + \mathcal{B}_\tau\bar{f}(\varepsilon(t - \tau(t))) + u(t), \quad (2.5a)$$

$$\bar{y}(t) = C\varepsilon(t), \quad (2.5b)$$

in which $\bar{f}(\varepsilon(t)) = f(\hat{x}(t)) - f(x(t))$.

In recent years, sampled-data control methods have been widely used in the literature [47–51]. Compared with sampled-data control methods, ETC methods can significantly reduce the update frequency of the controller, thereby saving computational and network resources. In the paper, the synchronization problem between drive-response TDNNs (2.1) and (2.3) is considered in the frame of SETC. The SETC mechanism adopted takes the form of

$$\alpha_{k+1} = \min \left\{ t \geq \alpha_k + \beta \mid (\bar{y}(t) - \bar{y}(\alpha_k))^T \Gamma (\bar{y}(t) - \bar{y}(\alpha_k)) \geq \epsilon \bar{y}^T(t) \Gamma \bar{y}(t) \right\}, \quad (2.6)$$

where α_k represents the k th triggering instant, $\Gamma \geq 0$ is called the trigger matrix and $\epsilon \geq 0$ and $\beta > 0$ are given scalars with β denoting the sensor waiting interval. That is, β means the shortest time between two adjacent event-triggering instances. According to the SETC mechanism (2.6) a controller can be recast as a control input subject to sampling for $t \in [\alpha_k, \alpha_k + \beta)$ and as a control input subject to continuous event triggering for $t \in [\alpha_k + \beta, \alpha_{k+1})$. Then, the control input takes the form of

$$u(t) = \begin{cases} -\bar{\mathcal{K}}C\varepsilon(t - \varrho(t)), & t \in [\alpha_k, \alpha_k + \beta), \\ -\bar{\mathcal{K}}[e(t) + C\varepsilon(t)], & t \in [\alpha_k + \beta, \alpha_{k+1}), \end{cases} \quad (2.7)$$

where

$$\varrho(t) = t - \alpha_k \leq \beta, \quad t \in [\alpha_k, \alpha_k + \beta), \quad (2.8)$$

$$e(t) = \bar{y}(\alpha_k) - \bar{y}(t), \quad t \in [\alpha_k + \beta, \alpha_{k+1}). \quad (2.9)$$

Remark 3. *The working mechanism of SETC is as follows. The sensor will wait β seconds after the k -th event is triggered at the instant α_k . When the time comes to the instant $\alpha_k + \beta$, it will begin to monitor the event-trigger condition continuously to determine the next triggering instant. Namely, once the judgment condition is true, the new measurement will be sent to update the controller at the instant α_{k+1} . Note that, in the case of $\epsilon = 0$, the SETC mechanism in (2.6) degenerates to the periodic sampled-data control mechanism.*

Hence, the error system can be constructed by using the system (2.5) and controller (2.7) as follows:

$$\dot{\varepsilon}(t) = -\mathcal{A}\varepsilon(t) + \mathcal{B}\bar{f}(\varepsilon(t)) + \mathcal{B}_\tau\bar{f}(\varepsilon(t - \tau(t))) - \bar{\mathcal{K}}C\varepsilon(t - \varrho(t)), \quad t \in [\alpha_k, \alpha_k + \beta), \quad (2.10a)$$

$$\dot{\varepsilon}(t) = (-\mathcal{A} - \bar{\mathcal{K}}C)\varepsilon(t) - \bar{\mathcal{K}}e(t) + \mathcal{B}\bar{f}(\varepsilon(t)) + \mathcal{B}_\tau\bar{f}(\varepsilon(t - \tau(t))), \quad t \in [\alpha_k + \beta, \alpha_{k+1}). \quad (2.10b)$$

To discuss the issue regarding the guaranteed cost index of the system in this paper, let us define

$$\mathcal{J}(t) = \int_0^t [\varepsilon^T(s)\mathcal{Q}\varepsilon(s) + u^T(s)\mathcal{R}u(s)] ds, \quad (2.11)$$

as a quadratic cost function, where $\mathcal{Q} > 0$ and $\mathcal{R} > 0$.

Next, we give a definition and some lemmas, which are required to gain our main results.

Definition 1. Consider the error system (2.10); if there exist a positive number \mathcal{J}° and an event-triggered control law $u(t)$ such that the error system is exponentially stable and the quadratic cost function (2.11) meets $\mathcal{J}(\infty) \leq \mathcal{J}^\circ$, then the control law $u(t)$ is called the cost-guaranteed controller and the upper-bound value \mathcal{J}° refers to the cost-related performance index.

Lemma 1. [52] Let $M > 0$ be an appropriate dimension matrix. Then, the inequality

$$\frac{1}{\mu_2 - \mu_1} \left[\int_{\mu_1}^{\mu_2} \vartheta(s) ds \right]^T M \left[\int_{\mu_1}^{\mu_2} \vartheta(s) ds \right] \leq \int_{\mu_1}^{\mu_2} \vartheta^T(s) M \vartheta(s) ds$$

holds, where the scalars μ_1 and μ_2 satisfy $\mu_2 > \mu_1$, and a vector function $\vartheta : [\mu_1, \mu_2] \rightarrow \mathbb{R}^n$.

Lemma 2. [53] For any matrices $M_1 \in \mathbb{R}^{n \times m}$, $M_2 \in \mathbb{R}^{n \times m}$, $M_3 = M_3^T > 0$, $M_3 \in \mathbb{R}^{n \times n}$, one can write

$$M_1^T M_2 + M_2^T M_1 \leq M_1^T M_3 M_1 + M_2^T M_3^{-1} M_2.$$

Lemma 3. [54] For any real matrices M_1, M_2, M_3 with appropriate dimensions,

$$\begin{bmatrix} M_1 & M_2 \\ * & M_3 \end{bmatrix} < 0$$

holds if and only if

$$M_3 < 0 \text{ and } M_1 - M_2 M_3^{-1} M_2^T < 0.$$

Before ending this section, let us clarify the purpose of this work, which was to design a SETC mechanism-based non-fragile cost-guaranteed controller to make sure that the error system in (2.10) is exponentially stable and the cost function in (2.11) satisfies $\mathcal{J}(\infty) \leq \mathcal{J}^\circ$.

3. Main results

3.1. Performance analysis

In the following, a criterion for the non-fragile exponential stability and cost-related performance under the conditions of the SETC mechanism is given.

Theorem 1. For the given scalars $\gamma > 0, \beta > 0, \epsilon \geq 0$, assume that there exist $p \times p$ matrices $P > 0, N > 0, S > 0, W, W_1, F_1, F_2, E_1, E_2, E_3, Y, p \times p$ diagonal matrices $U > 0, \Lambda_1 > 0, \Lambda_2 > 0$, and a $q \times q$ matrix $\Gamma \geq 0$ such that

$$F > 0, \Theta_0 < 0, \Theta_1 < 0, \Phi < 0, \quad (3.1)$$

in which

$$F = \begin{bmatrix} P + \beta \frac{W+W^T}{2} & -\beta W + \beta W_1 \\ * & -\beta W_1 - \beta W_1^T + \beta \frac{W+W^T}{2} \end{bmatrix}, \quad (3.2)$$

$$\Theta_0 = \begin{bmatrix} \Theta_{11} - W_\gamma & \Theta_{12} + \beta \frac{W+W^T}{2} & \Theta_{13} + \hat{W}_{1\gamma} & \Psi_1 & 0 & F_1^T \mathcal{B}_\tau \\ * & \Theta_{22} + \beta N & \Theta_{23} - \beta(W - W_1) & \Psi_2 & 0 & F_2^T \mathcal{B}_\tau \\ * & * & \Theta_{33} - \hat{W}_{2\gamma} & 0 & 0 & 0 \\ * & * & * & -2\Lambda_1 & 0 & 0 \\ * & * & * & * & \Psi_3 & L\Lambda_2 \\ * & * & * & * & * & -2\Lambda_2 \end{bmatrix}, \quad (3.3)$$

$$\Theta_1 = \begin{bmatrix} \Theta_{11} - \frac{W+W^T}{2} & \Theta_{12} & \Theta_{13} + \check{W}_{1\gamma} & \beta E_1^T & \Psi_1 & 0 & F_1^T \mathcal{B}_\tau \\ * & \Theta_{22} & \Theta_{23} & \beta E_2^T & \Psi_2 & 0 & F_2^T \mathcal{B}_\tau \\ * & * & \Theta_{33} - \check{W}_{2\gamma} & \beta E_3^T & 0 & 0 & 0 \\ * & * & * & -\beta e^{-2\gamma\beta} N & 0 & 0 & 0 \\ * & * & * & * & -2\Lambda_1 & 0 & 0 \\ * & * & * & * & * & \Psi_3 & L\Lambda_2 \\ * & * & * & * & * & * & -2\Lambda_2 \end{bmatrix}, \quad (3.4)$$

$$\Phi = \begin{bmatrix} \Phi_{11} & \Phi_{12} & -F_1^T \bar{\mathcal{K}} + C^T \bar{\mathcal{K}}^T \mathcal{R} \bar{\mathcal{K}} & \Psi_1 & 0 & F_1^T \mathcal{B}_\tau \\ * & -F_2^T - F_2 & -F_2^T \bar{\mathcal{K}} & \Psi_2 & 0 & F_2^T \mathcal{B}_\tau \\ * & * & -\Gamma + \bar{\mathcal{K}}^T \mathcal{R} \bar{\mathcal{K}} & 0 & 0 & 0 \\ * & * & * & -2\Lambda_1 & 0 & 0 \\ * & * & * & * & \Psi_3 & L\Lambda_2 \\ * & * & * & * & * & -2\Lambda_2 \end{bmatrix}, \quad (3.5)$$

with

$$\begin{aligned} \Theta_{11} &= -F_1^T \mathcal{A} - \mathcal{A}^T F_1 - E_1^T - E_1 + 2\gamma P + 2\gamma UL + S + Q, \\ \Theta_{12} &= P - F_1^T - \mathcal{A}^T F_2 - E_2, \\ \Theta_{13} &= -E_3 - F_1^T KC + E_1^T, \\ \Theta_{22} &= -F_2 - F_2^T, \\ \Theta_{23} &= -F_2^T \bar{\mathcal{K}} C + E_2^T, \\ \Theta_{33} &= E_3 + E_3^T + C^T \bar{\mathcal{K}}^T \mathcal{R} \bar{\mathcal{K}} C, \\ \Psi_1 &= F_1^T \mathcal{B} + L\Lambda_1, \quad \Psi_2 = F_2^T \mathcal{B} + U, \quad \Psi_3 = (\mu - 1)e^{-2\gamma\tau} S, \\ U &= \text{diag}\{u_1, u_2, \dots, u_p\}, \\ W_\gamma &= (1/2 - \gamma\beta)(W + W^T), \\ \hat{W}_{1\gamma} &= (1 - 2\gamma\beta)(W - W_1), \\ \check{W}_{1\gamma} &= W - W_1, \\ \hat{W}_{2\gamma} &= (1/2 - \gamma\beta)(W + W^T - 2W_1 - 2W_1^T), \\ \check{W}_{2\gamma} &= (1/2)(W + W^T - 2W_1 - 2W_1^T), \end{aligned}$$

$$\begin{aligned}\Phi_{11} &= F_1^T(-\mathcal{A} - \bar{\mathcal{K}}C) + (-\mathcal{A} - \bar{\mathcal{K}}C)^T F_1 + \epsilon C^T \Gamma C + 2\gamma P \\ &\quad + C^T \bar{\mathcal{K}}^T \mathcal{R} \bar{\mathcal{K}} C + 2\gamma UL + S + Q, \\ \Phi_{12} &= P + (-\mathcal{A} - \bar{\mathcal{K}}C)^T F_2 - F_1^T.\end{aligned}$$

Then, the system (2.10) remains exponentially stable and the cost function in (2.11) satisfies $\mathcal{J}(\infty) \leq \epsilon^T(0)(P + UL)\epsilon(0) + \int_{-\tau}^0 \epsilon^T(s)S\epsilon(s)ds$.

Proof. Let us choose a time-dependent Lyapunov functional as

$$\mathcal{V}(t) = \begin{cases} \mathcal{V}_1(t), & t \in [\alpha_k, \alpha_k + \beta), \\ \mathcal{V}_2(t), & t \in [\alpha_k + \beta, \alpha_{k+1}), \end{cases} \quad (3.6)$$

in which $\mathcal{V}_1(t) = \mathcal{V}_P(t) + \mathcal{V}_U(t) + \mathcal{V}_S(t) + \mathcal{V}_N(t) + \mathcal{V}_W(t)$, $\mathcal{V}_2(t) = \mathcal{V}_P(t) + \mathcal{V}_U(t) + \mathcal{V}_S(t)$ with

$$\begin{aligned}\mathcal{V}_P(t) &= \epsilon^T(t)P\epsilon(t), \\ \mathcal{V}_U(t) &= 2 \sum_{i=1}^n u_i \int_0^{\epsilon_i(t)} \bar{f}_i(s)ds, \\ \mathcal{V}_S(t) &= \int_{t-\tau(t)}^t e^{2\gamma(s-t)} \epsilon^T(s)S\epsilon(s)ds, \\ \mathcal{V}_N(t) &= (\beta - \varrho(t)) \int_{t-\varrho(t)}^t e^{2\gamma(s-t)} \dot{\epsilon}^T(s)N\dot{\epsilon}(s)ds, \\ \mathcal{V}_W(t) &= (\beta - \varrho(t))\psi^T(t) \begin{bmatrix} \frac{W+W^T}{2} & -W + W_1 \\ * & -W_1 - W_1^T + \frac{W+W^T}{2} \end{bmatrix} \psi(t),\end{aligned}$$

where $\psi(t) = \text{col}\{\epsilon(t), \epsilon(t - \varrho(t))\}$. Clearly, $\mathcal{V}(t)$ is continuous on $[0, +\infty)$.

Note that the linear matrix inequality (LMI) (3.2) can ensure that $V_P(t) + V_W(t)$ is positive definite, as follows:

$$\begin{aligned}&\mathcal{V}_P(t) + \mathcal{V}_W(t) \\ &= \epsilon^T(t)P\epsilon(t) + (\beta - \varrho(t))\psi^T(t) \begin{bmatrix} \frac{W+W^T}{2} & -W + W_1 \\ * & -W_1 - W_1^T + \frac{W+W^T}{2} \end{bmatrix} \psi(t) \\ &= \psi^T(t) \begin{bmatrix} P + (\beta - \varrho(t))\frac{W+W^T}{2} & (\beta - \varrho(t))(-W + W_1) \\ * & (\beta - \varrho(t))(-W_1 - W_1^T + \frac{W+W^T}{2}) \end{bmatrix} \psi(t) \\ &= \left(\frac{\beta - \varrho(t)}{\beta}\right)\psi^T(t)F\psi(t) + \left(\frac{\varrho(t)}{\beta}\right)\psi^T(t) \begin{bmatrix} P & 0 \\ * & 0 \end{bmatrix} \psi(t).\end{aligned} \quad (3.7)$$

Owing to $F > 0$ and $P > 0$, it follows from (3.6) and (3.7) that

$$\min\{\lambda_{\min}(P), \lambda_{\min}(F)\} \|\epsilon(t)\|^2 \leq \mathcal{V}(t). \quad (3.8)$$

Taking the time derivative of the above functions along the trajectories of the system (2.10), it is not hard to derive that

$$\dot{\mathcal{V}}_P(t) = 2\epsilon^T(t)P\dot{\epsilon}(t), \quad (3.9)$$

$$\dot{\mathcal{V}}_U(t) = 2\bar{f}^T(\varepsilon(t))U\dot{\varepsilon}(t), \quad (3.10)$$

$$\begin{aligned} \dot{\mathcal{V}}_S(t) &= -2\gamma\mathcal{V}_S(t) + \varepsilon^T(t)S\varepsilon(t) - (1 - \dot{\tau}(t)) \times e^{-2\gamma\tau(t)}\varepsilon^T(t - \tau(t))S\varepsilon(t - \tau(t)) \\ &\leq -2\gamma\mathcal{V}_S(t) + \varepsilon^T(t)S\varepsilon(t) - (1 - \mu) \times e^{-2\gamma\tau} \varepsilon^T(t - \tau(t))S\varepsilon(t - \tau(t)) \end{aligned} \quad (3.11)$$

$$\begin{aligned} \dot{\mathcal{V}}_N(t) &= - \int_{t-\varrho(t)}^t e^{2\gamma(s-t)}\dot{\varepsilon}^T(s)N\dot{\varepsilon}(s)ds - 2\gamma(\beta - \varrho(t)) \int_{t-\varrho(t)}^t e^{2\gamma(s-t)}\dot{\varepsilon}^T(s)N\dot{\varepsilon}(s)ds \\ &\quad + (\beta - \varrho(t))\dot{\varepsilon}^T(t)N\dot{\varepsilon}(t) \\ &\leq - \int_{t-\varrho(t)}^t e^{-2\gamma\beta}\dot{\varepsilon}^T(s)N\dot{\varepsilon}(s)ds - 2\gamma(\beta - \varrho(t)) \int_{t-\varrho(t)}^t e^{2\gamma(s-t)}\dot{\varepsilon}^T(s)N\dot{\varepsilon}(s)ds \\ &\quad + (\beta - \varrho(t))\dot{\varepsilon}^T(t)N\dot{\varepsilon}(t), \end{aligned} \quad (3.12)$$

$$\begin{aligned} \dot{\mathcal{V}}_W(t) &= -\psi^T(t) \begin{bmatrix} \frac{W+W^T}{2} & -W + W_1 \\ * & -W_1 - W_1^T + \frac{W+W^T}{2} \end{bmatrix} \psi(t) \\ &\quad + (\beta - \varrho(t))[\dot{\varepsilon}^T(t)(W + W^T)\varepsilon(t) + 2\dot{\varepsilon}^T(t)(-W + W_1)\varepsilon(t - \varrho(t))]. \end{aligned} \quad (3.13)$$

The proof can be divided into two cases in the light of the segmented time periods as follows.

Case I: With respect to $t \in [\alpha_k, \alpha_k + \beta)$, the Lyapunov functional $\mathcal{V}_1(t)$ can be adopted for the system (2.10a).

Denote

$$z_1 = \frac{1}{\varrho(t)} \int_{t-\varrho(t)}^t \dot{\varepsilon}(s)ds.$$

Applying Lemma 1 to the first term of (3.12), it can be acquired that

$$-e^{-2\gamma\beta} \int_{t-\varrho(t)}^t \dot{\varepsilon}^T(s)N\dot{\varepsilon}(s)ds \leq -\varrho(t)e^{-2\gamma\beta}z_1^T N z_1. \quad (3.14)$$

For free-weighting matrices E_1, E_2, E_3, F_1 and F_2 with proper dimensions, the following expressions hold:

$$0 = 2 \left[\varepsilon^T(t)E_1^T + \dot{\varepsilon}^T(t)E_2^T + \varepsilon^T(t - \varrho(t))E_3^T \right] [\varrho(t)z_1 + \varepsilon(t - \varrho(t)) - \varepsilon(t)], \quad (3.15)$$

$$0 = 2 \left[\varepsilon^T(t)F_1^T + \dot{\varepsilon}^T(t)F_2^T \right] [-\mathcal{A}\varepsilon(t) - \bar{\mathcal{K}}C\varepsilon(t - \varrho(t)) + \mathcal{B}\bar{f}(\varepsilon(t)) + \mathcal{B}_\tau\bar{f}(\varepsilon(t - \tau(t))) - \dot{\varepsilon}(t)]. \quad (3.16)$$

In view of Assumption 1, for any diagonal matrix $\Lambda_1 > 0$ and $\Lambda_2 > 0$, it follows that

$$0 \leq -2\bar{f}^T(\varepsilon(t))\Lambda_1\bar{f}(\varepsilon(t)) + 2\varepsilon^T(t)L\Lambda_1\bar{f}(\varepsilon(t)), \quad (3.17)$$

$$0 \leq -2\bar{f}^T(\varepsilon(t - \tau(t)))\Lambda_2\bar{f}(\varepsilon(t - \tau(t))) + 2\varepsilon^T(t - \tau(t))L\Lambda_2\bar{f}(\varepsilon(t - \tau(t))). \quad (3.18)$$

According to Assumption 1, we can also obtain

$$0 \leq \int_0^{\varepsilon_i(t)} \bar{f}_i(s)ds \leq \frac{1}{2}\varepsilon_i^2(t)L_i.$$

Then, we have

$$2 \sum_{i=1}^n \omega_i \int_0^{\varepsilon_i(t)} \bar{f}_i(s)ds$$

$$\begin{aligned}
&\leq 2(\omega_1 \frac{1}{2} \varepsilon_1^2(t) L_1 + \cdots + \omega_n \frac{1}{2} \varepsilon_n^2(t) L_n) \\
&= \varepsilon^T(t) U L \varepsilon(t).
\end{aligned} \tag{3.19}$$

By summing up (3.9)–(3.12) and (3.15)–(3.19) and using (3.14), we find that

$$\begin{aligned}
&\dot{\mathcal{V}}_1(t) + 2\gamma \mathcal{V}_1(t) + \varepsilon^T(t) Q \varepsilon(t) + \varepsilon^T(t - \varrho(t)) C^T \bar{\mathcal{K}}^T \mathcal{R} \bar{\mathcal{K}} C \varepsilon(t - \varrho(t)) \\
\leq & 2\varepsilon^T(t) P \dot{\varepsilon}(t) + 2\gamma \varepsilon^T(t) P \varepsilon(t) + 2\bar{f}^T(\varepsilon(t)) U \dot{\varepsilon}(t) + 2\gamma \varepsilon^T(t) U L \varepsilon(t) \\
& + \varepsilon^T(t) S \varepsilon(t) - (1 - \mu) \times e^{-2\gamma\tau} \varepsilon^T(t - \tau(t)) S \varepsilon(t - \tau(t)) \\
& - \varrho(t) e^{-2\gamma\beta} z_1^T N z_1 + (\beta - \varrho(t)) \dot{\varepsilon}^T(t) N \dot{\varepsilon}(t) - \varepsilon^T(t) \left(\frac{W + W^T}{2} \right) \varepsilon(t) \\
& - \varepsilon^T(t - \varrho(t)) (-W + W_1)^T \varepsilon(t) - \varepsilon^T(t) (-W + W_1) \varepsilon(t - \varrho(t)) \\
& - \varepsilon^T(t - \varrho(t)) (-W_1 - W_1^T + \frac{W + W^T}{2}) \varepsilon(t - \varrho(t)) \\
& + \dot{\varepsilon}^T(t) (\beta - \varrho(t)) (W + W^T) \varepsilon(t) + 2\dot{\varepsilon}^T(t) (\beta - \varrho(t)) (-W + W_1) \varepsilon(t - \varrho(t)) \\
& + 2\gamma (\beta - \varrho(t)) \psi^T(t) \begin{bmatrix} \frac{W+W^T}{2} & -W+W_1 \\ * & -W_1-W_1^T+\frac{W+W^T}{2} \end{bmatrix} \psi(t) + 2(\varepsilon^T(t) E_1^T \varrho(t) z_1 \\
& + \dot{\varepsilon}^T(t) E_2^T \varrho(t) z_1 + \varepsilon^T(t - \varrho(t)) E_3^T \varrho(t) z_1 + \varepsilon^T(t) E_1^T \varepsilon(t - \varrho(t)) + \dot{\varepsilon}^T(t) E_2^T \varepsilon(t - \varrho(t)) \\
& + \varepsilon^T(t - \varrho(t)) E_3^T \varepsilon(t - \varrho(t)) - \varepsilon^T(t) E_1^T \varepsilon(t) - \dot{\varepsilon}^T(t) E_2^T \varepsilon(t) - \varepsilon^T(t - \varrho(t)) E_3^T \varepsilon(t)) \\
& + 2(-\varepsilon^T(t) F_1^T \mathcal{A} \varepsilon(t) - \dot{\varepsilon}^T(t) F_2^T \mathcal{A} \varepsilon(t) - \varepsilon^T(t) F_1^T \bar{\mathcal{K}} C \varepsilon(t - \varrho(t)) - \dot{\varepsilon}^T(t) F_2^T \bar{\mathcal{K}} C \varepsilon(t - \varrho(t)) \\
& + \varepsilon^T(t) F_1^T \mathcal{B} \bar{f}(\varepsilon(t)) + \dot{\varepsilon}^T(t) F_2^T \mathcal{B} \bar{f}(\varepsilon(t)) + \varepsilon^T(t) F_1^T \mathcal{B}_\tau \bar{f}(\varepsilon(t - \tau(t))) \\
& + \dot{\varepsilon}^T(t) F_2^T \mathcal{B}_\tau \bar{f}(\varepsilon(t - \tau(t))) - \varepsilon^T(t) F_1^T \dot{\varepsilon}(t) - \dot{\varepsilon}^T(t) F_2^T \dot{\varepsilon}(t)) \\
& - 2\bar{f}^T(\varepsilon(t)) \Lambda_1 \bar{f}(\varepsilon(t)) + 2\varepsilon^T(t) L \Lambda_1 \bar{f}(\varepsilon(t)) \\
& - 2\bar{f}^T(\varepsilon(t - \tau(t))) \Lambda_2 \bar{f}(\varepsilon(t - \tau(t))) + 2\varepsilon^T(t - \tau(t)) L \Lambda_2 \bar{f}(\varepsilon(t - \tau(t))) \\
& + \varepsilon^T(t) Q \varepsilon(t) + \varepsilon^T(t - \varrho(t)) C^T \bar{\mathcal{K}}^T \mathcal{R} \bar{\mathcal{K}} C \varepsilon(t - \varrho(t)) \\
= & \frac{\beta - \varrho(t)}{\beta} \eta_1^T(t) \Theta_0 \eta_1(t) + \frac{\varrho(t)}{\beta} \eta_2^T(t) \Theta_1 \eta_2(t),
\end{aligned}$$

where $\eta_1^T(t) = \{\varepsilon^T(t), \dot{\varepsilon}^T(t), \varepsilon^T(t - \varrho(t)), \bar{f}^T(\varepsilon(t)), \varepsilon^T(t - \tau(t)), \bar{f}^T(\varepsilon(t - \tau(t)))\}$ and $\eta_2^T(t) = \{\varepsilon^T(t), \dot{\varepsilon}^T(t), \varepsilon^T(t - \varrho(t)), z_1^T, \bar{f}^T(\varepsilon(t)), \varepsilon^T(t - \tau(t)), \bar{f}^T(\varepsilon(t - \tau(t)))\}$. Then, the conditions $\Theta_0 < 0$ and $\Theta_1 < 0$ can ensure that

$$\dot{\mathcal{V}}_1(t) + 2\gamma \mathcal{V}_1(t) \leq -\varepsilon^T(t) Q \varepsilon(t) - \varepsilon^T(t - \varrho(t)) C^T \bar{\mathcal{K}}^T \mathcal{R} \bar{\mathcal{K}} C \varepsilon(t - \varrho(t)) \leq 0, \quad t \in [\alpha_k, \alpha_k + \beta). \tag{3.20}$$

Case 2: With respect to $t \in [\alpha_k + \beta, \alpha_{k+1})$, we employ the Lyapunov functional $\mathcal{V}_2(t)$ for the system (2.10b). Similar to (3.16), applying the free-weighting matrix approach, one can gain

$$0 = 2 \left[\varepsilon^T(t) F_1^T + \dot{\varepsilon}^T(t) F_2^T \right] [(-\mathcal{A} - \bar{\mathcal{K}} C) \varepsilon(t) - \bar{\mathcal{K}} e(t) + \mathcal{B} \bar{f}(\varepsilon(t)) + \mathcal{B}_\tau \bar{f}(\varepsilon(t - \tau(t))) - \dot{\varepsilon}(t)]. \tag{3.21}$$

In view of the event-triggering condition (2.6), one easily obtains that

$$0 \leq -e^T(t) \Gamma e(t) + \epsilon [C \varepsilon(t)]^T \Gamma [C \varepsilon(t)]. \tag{3.22}$$

In view of Assumption 1, for any diagonal matrix $\Lambda_1 > 0$ and $\Lambda_2 > 0$, it follows that

$$0 \leq -2\bar{f}^T(\varepsilon(t))\Lambda_1\bar{f}(\varepsilon(t)) + 2\varepsilon^T(t)L\Lambda_1\bar{f}(\varepsilon(t)) \quad (3.23)$$

$$0 \leq -2\bar{f}^T(\varepsilon(t - \tau(t)))\Lambda_2\bar{f}(\varepsilon(t - \tau(t))) + 2\varepsilon^T(t - \tau(t))L\Lambda_2\bar{f}(\varepsilon(t - \tau(t))) \quad (3.24)$$

By summing up (3.9), (3.10), (3.19) and (3.21)–(3.24), we find that

$$\begin{aligned} & \dot{\mathcal{V}}_2(t) + 2\gamma\mathcal{V}_2(t) + \varepsilon^T(t)\mathcal{Q}\varepsilon(t) + [\bar{\mathcal{K}}(e(t) + C\varepsilon(t))]^T\mathcal{R}[\bar{\mathcal{K}}(e(t) + C\varepsilon(t))] \\ \leq & 2\varepsilon^T(t)P\dot{\varepsilon}(t) + 2\gamma\varepsilon^T(t)P\varepsilon(t) + 2\bar{f}^T(\varepsilon(t))U\dot{\varepsilon}(t) + 2\gamma\varepsilon^T(t)UL\varepsilon(t) \\ & + \varepsilon^T(t)S\varepsilon(t) - (1 - \mu) \times e^{-2\gamma\tau} \varepsilon^T(t - \tau(t))S\varepsilon(t - \tau(t)) \\ & + 2(\varepsilon^T(t)F_1^T(-\mathcal{A} - \bar{\mathcal{K}}C)\varepsilon(t) + \dot{\varepsilon}^T(t)F_2^T(-\mathcal{A} - \bar{\mathcal{K}}C)\varepsilon(t) - \varepsilon^T(t)F_1^T\bar{\mathcal{K}}e(t) - \dot{\varepsilon}^T(t)F_2^T\bar{\mathcal{K}}e(t) \\ & + \varepsilon^T(t)F_1^T\mathcal{B}\bar{f}(\varepsilon(t)) + \dot{\varepsilon}^T(t)F_2^T\mathcal{B}\bar{f}(\varepsilon(t)) + \varepsilon^T(t)F_1^T\mathcal{B}_\tau\bar{f}(\varepsilon(t - \tau(t))) + \dot{\varepsilon}^T(t)F_2^T\mathcal{B}_\tau\bar{f}(\varepsilon(t - \tau(t))) \\ & - \varepsilon^T(t)F_1^T\dot{\varepsilon}(t) - \dot{\varepsilon}^T(t)F_2^T\dot{\varepsilon}(t)) \\ & + \varepsilon\varepsilon^T(t)C^T\Gamma C\varepsilon(t) - e^T(t)\Gamma e(t) - 2\bar{f}^T(\varepsilon(t))\Lambda_1\bar{f}(\varepsilon(t)) + 2\varepsilon^T(t)L\Lambda_1\bar{f}(\varepsilon(t)) \\ & - 2\bar{f}^T(\varepsilon(t - \tau(t)))\Lambda_2\bar{f}(\varepsilon(t - \tau(t))) + 2\varepsilon^T(t - \tau(t))L\Lambda_2\bar{f}(\varepsilon(t - \tau(t))) \\ & + \varepsilon^T(t)\mathcal{Q}\varepsilon(t) + [\bar{\mathcal{K}}(e(t) + C\varepsilon(t))]^T\mathcal{R}[\bar{\mathcal{K}}(e(t) + C\varepsilon(t))] \\ = & \eta_3^T(t)\Phi\eta_3(t), \end{aligned}$$

where $\eta_3^T(t) = \{\varepsilon^T(t), \dot{\varepsilon}^T(t), e^T(t), \bar{f}^T(\varepsilon(t)), \varepsilon^T(t - \tau(t)), \bar{f}^T(\varepsilon(t - \tau(t)))\}$. Similarly, the condition $\Phi < 0$ implies

$$\dot{\mathcal{V}}_2(t) + 2\gamma\mathcal{V}_2(t) \leq -\varepsilon^T(t)\mathcal{Q}\varepsilon(t) - [\bar{\mathcal{K}}(e(t) + C\varepsilon(t))]^T\mathcal{R}[\bar{\mathcal{K}}(e(t) + C\varepsilon(t))] \leq 0, \quad t \in [\alpha_k + \beta, \alpha_{k+1}). \quad (3.25)$$

From (3.20) and (3.25), it can be concluded that

$$\dot{\mathcal{V}}(t) + 2\gamma\mathcal{V}(t) \leq 0$$

for any $t \in [\alpha_k, \alpha_{k+1})$. Especially, for $t \in [\alpha_k + \beta, \alpha_{k+1})$, integrating over (3.25) with respect to t , one can get

$$\begin{aligned} \mathcal{V}(t) & \leq \mathcal{V}(\alpha_k + \beta)e^{-2\gamma(t - \alpha_k - \beta)} \leq \mathcal{V}(\alpha_k)e^{-2\gamma(t - \alpha_k)} \\ & \leq \mathcal{V}(\alpha_{k-1} + \beta)e^{-2\gamma(t - \alpha_{k-1} - \beta)} \leq \mathcal{V}(\alpha_{k-1})e^{-2\gamma(t - \alpha_{k-1})} \\ & \leq \dots \leq \mathcal{V}(0)e^{-2\gamma t}. \end{aligned}$$

For $t \in [\alpha_k, \alpha_k + \beta)$, by a similar procedure as above, we can derive the same result from the inequality (3.20). Therefore, we have

$$\mathcal{V}(t) \leq \mathcal{V}(0)e^{-2\gamma t}. \quad (3.26)$$

From (3.8) and (3.26) we get

$$\|\varepsilon(t)\| \leq \sqrt{\frac{\mathcal{V}(0)}{\min\{\lambda_{\min}(P), \lambda_{\min}(F)\}}} e^{-\gamma t}.$$

Thus, the system in Eq (2.10) is exponentially stable. In addition, since $\mathcal{V}(t) \geq 0$ and $\gamma > 0$, combining (3.20) with (3.25), we can write

$$\dot{\mathcal{V}}(t) \leq -\varepsilon^T(t)Q\varepsilon(t) - u^T(t)\mathcal{R}u(t).$$

It follows immediately that

$$\mathcal{J}(\infty) \leq \int_0^\infty -\dot{\mathcal{V}}(t)dt \leq \mathcal{V}(0) \leq \varepsilon^T(0)(P + UL)\varepsilon(0) + \int_{-\tau}^0 \varepsilon^T(s)S\varepsilon(s)ds. \quad (3.27)$$

This finishes the proof. \square

Remark 4. The synchronization-error system composed of (2.10) and (2.7) is actually a switched system over the sampling interval under SETC mechanism (2.6). To match the switched system, a piecewise functional $\mathcal{V}(t)$ is constructed; it switches between the functions $\mathcal{V}_1(t)$ and $\mathcal{V}_2(t)$. Specifically, for the waiting time interval, the time-dependent functional $\mathcal{V}_1(t)$ is applied, while for the continuous event detection interval, the time-independent functional $\mathcal{V}_2(t)$ is employed. The function constructed not only fully utilizes the available state information, but also the activation function information on the interval $[\alpha_k, \alpha_{k+1}]$.

3.2. Design method

This subsection gives a joint design of the event-trigger matrix Γ in (2.6) and the desired non-fragile controller gain \mathcal{K} for the system (2.10).

Theorem 2. For the given scalars $\kappa, \gamma > 0, \beta > 0, \epsilon \geq 0$, suppose that there exist $p \times p$ matrices $P > 0, N > 0, S > 0, W, W_1, F_1, E_1, E_2, E_3, Y, p \times p$ diagonal matrices $U > 0, \Lambda_1 > 0, \Lambda_2 > 0$, a $q \times q$ matrix $\Gamma \geq 0$, and scalars $\alpha_0 > 0$ and $\alpha_1 > 0$ such that

$$F > 0, \Theta_0^* < 0, \Theta_1^* < 0, \Phi^* < 0, \quad (3.28)$$

where F is given in Theorem 1, and

$$\Theta_0^* = \begin{bmatrix} \Xi_{11} & \Xi_{12} & \Xi_{13} & \Psi_1 & 0 & F_1^T \mathcal{B}_\tau & 0 & -F_1^T \mathcal{G} \\ * & \Xi_{22} & \Xi_{23} & \tilde{\Psi}_2 & 0 & \kappa F_1^T \mathcal{B}_\tau & 0 & -\kappa F_1^T \mathcal{G} \\ * & * & \Xi_{33} & 0 & 0 & 0 & C^T Y^T & 0 \\ * & * & * & -2\Lambda_1 & 0 & 0 & 0 & 0 \\ * & * & * & * & \Psi_3 & L\Lambda_2 & 0 & 0 \\ * & * & * & * & * & -2\Lambda_2 & 0 & 0 \\ * & * & * & * & * & * & \Psi_4 & \mathcal{G} \\ * & * & * & * & * & * & * & -\alpha_0 I \end{bmatrix}, \quad (3.29)$$

$$\Theta_1^* = \begin{bmatrix} \Pi_{11} & \Pi_{12} & \Pi_{13} & \beta E_1^T & \Psi_1 & 0 & F_1^T \mathcal{B}_\tau & 0 & -F_1^T \mathcal{G} \\ * & \Pi_{22} & \Pi_{23} & \beta E_2^T & \tilde{\Psi}_2 & 0 & \kappa F_1^T \mathcal{B}_\tau & 0 & -\kappa F_1^T \mathcal{G} \\ * & * & \Pi_{33} & \beta E_3^T & 0 & 0 & 0 & C^T Y^T & 0 \\ * & * & * & -\beta e^{-2\gamma\beta} N & 0 & 0 & 0 & 0 & 0 \\ * & * & * & * & -2\Lambda_1 & 0 & 0 & 0 & 0 \\ * & * & * & * & * & \Psi_3 & L\Lambda_2 & 0 & 0 \\ * & * & * & * & * & * & -2\Lambda_2 & 0 & 0 \\ * & * & * & * & * & * & * & \Psi_4 & \mathcal{G} \\ * & * & * & * & * & * & * & * & -\alpha_0 I \end{bmatrix}, \quad (3.30)$$

$$\Phi^* = \begin{bmatrix} \Sigma_{11} & \Sigma_{12} & \Sigma_{13} & \Psi_1 & 0 & F_1^T \mathcal{B}_\tau & C^T Y^T & -F_1^T \mathcal{G} \\ * & \Sigma_{22} & -\kappa Y & \tilde{\Psi}_2 & 0 & \kappa F_1^T \mathcal{B}_\tau & 0 & -\kappa F_1^T \mathcal{G} \\ * & * & \Sigma_{33} & 0 & 0 & 0 & Y^T & 0 \\ * & * & * & -2\Lambda_1 & 0 & 0 & 0 & 0 \\ * & * & * & * & \Psi_3 & L\Lambda_2 & 0 & 0 \\ * & * & * & * & * & -2\Lambda_2 & 0 & 0 \\ * & * & * & * & * & * & \Psi_4 & \mathcal{G} \\ * & * & * & * & * & * & * & -\alpha_1 I \end{bmatrix}, \quad (3.31)$$

with

$$\begin{aligned} \Xi_{11} &= -(1/2 - \gamma\beta)(W + W^T) - F_1^T \mathcal{A} - \mathcal{A}^T F_1 \\ &\quad - E_1^T - E_1 + 2\gamma P + 2\gamma UL + S + Q, \\ \Xi_{12} &= \beta \frac{W + W^T}{2} + P - F_1^T - \kappa \mathcal{A}^T F_1 - E_2, \\ \Xi_{13} &= (1 - 2\gamma\beta)(W - W_1) + E_1^T - YC - E_3, \\ \Xi_{22} &= -\kappa F_1^T - \kappa F_1 + \beta N, \\ \Xi_{23} &= E_2^T - \kappa YC - \beta(W - W_1), \\ \Xi_{33} &= E_3 + E_3^T + \alpha_0 C^T \mathcal{M}^T \mathcal{M} C - (1/2 - \gamma\beta)(W + W^T - 2W_1 - 2W_1^T), \\ \Pi_{11} &= -\frac{W + W^T}{2} - F_1^T \mathcal{A} - \mathcal{A}^T F_1 + 2\gamma UL + S + Q \\ &\quad - E_1^T - E_1 + 2\gamma P, \\ \Pi_{12} &= P - F_1^T - \kappa \mathcal{A}^T F_1 - E_2, \\ \Pi_{13} &= E_1^T - YC - E_3 + W - W_1, \\ \Pi_{22} &= -\kappa F_1^T - \kappa F_1, \\ \Pi_{23} &= E_2^T - \kappa YC, \\ \Pi_{33} &= E_3 + E_3^T + \alpha_0 C^T \mathcal{M}^T \mathcal{M} C - (1/2)(W + W^T - 2W_1 - 2W_1^T), \\ \Sigma_{11} &= -F_1^T \mathcal{A} - \mathcal{A}^T F_1 - YC - C^T Y^T + \epsilon C^T \Gamma C \\ &\quad + 2\gamma P + 2\gamma UL + S + Q + \alpha_1 C^T \mathcal{M}^T \mathcal{M} C, \\ \Sigma_{12} &= P - \kappa \mathcal{A}^T F_1 - \kappa C^T Y^T - F_1^T, \\ \Sigma_{13} &= -Y + \alpha_1 C^T \mathcal{M}^T \mathcal{M}, \\ \Sigma_{22} &= -\kappa F_1^T - \kappa F_1, \\ \Sigma_{33} &= -\Gamma + \alpha_1 \mathcal{M}^T \mathcal{M}, \\ \tilde{\Psi}_2 &= \kappa F_1^T \mathcal{B} + U, \\ \Psi_4 &= -\vartheta F_1 - \vartheta F_1^T + \vartheta^2 \mathcal{R}, \end{aligned}$$

and the other notations are the same as those in Theorem 1. Then, the proposed controller (2.7) with the gain matrix

$$\mathcal{K} = (F_1^T)^{-1} Y \quad (3.32)$$

exponentially stabilizes the error system (2.10) under the conditions of the SETC mechanism, and the cost function in (2.11) satisfies $\mathcal{J}(\infty) \leq \varepsilon^T(0)(P + UL)\varepsilon(0) + \int_{-\tau}^0 \varepsilon^T(s)S\varepsilon(s)ds$.

Proof. According to (2.4) and Lemma 3, (3.5) is equivalent to

$$\Phi = \check{\Phi} + He(\Upsilon_1 \mathcal{T}(t) \Upsilon_2)$$

where

$$\check{\Phi} = \begin{bmatrix} \check{\Sigma}_{11} & \check{\Sigma}_{12} & -F_1^T \mathcal{K} & \Psi_1 & 0 & F_1^T \mathcal{B}_\tau & C^T \mathcal{K}^T \\ * & -F_2^T - F_2 & -F_2^T \mathcal{K} & \Psi_2 & 0 & F_2^T \mathcal{B}_\tau & 0 \\ * & * & -\Gamma & 0 & 0 & 0 & \mathcal{K}^T \\ * & * & * & -2\Lambda_1 & 0 & 0 & 0 \\ * & * & * & * & \Psi_3 & L\Lambda_2 & 0 \\ * & * & * & * & * & -2\Lambda_2 & 0 \\ * & * & * & * & * & * & -\mathcal{R}^{-1} \end{bmatrix},$$

with

$$\begin{aligned} \check{\Sigma}_{11} &= F_1^T(-\mathcal{A} - \mathcal{K}C) + (-\mathcal{A} - \mathcal{K}C)^T F_1 + \epsilon C^T \Gamma C \\ &\quad + 2\gamma P + 2\gamma UL + S + Q, \\ \check{\Sigma}_{12} &= P + (-\mathcal{A} - \mathcal{K}C)^T F_2 - F_1^T, \\ \Upsilon_1 &= \begin{bmatrix} -\mathcal{G}^T F_1 & -\mathcal{G}^T F_2 & 0 & 0 & 0 & 0 & \mathcal{G}^T \end{bmatrix}^T, \\ \Upsilon_2 &= \begin{bmatrix} \mathcal{M}C & 0 & \mathcal{M} & 0 & 0 & 0 & 0 \end{bmatrix}. \end{aligned}$$

By using Lemma 2 and (2.4), we have

$$He(\Upsilon_1 \mathcal{T}(t) \Upsilon_2) \leq \frac{1}{\alpha_1} \Upsilon_1 \Upsilon_1^T + \alpha_1 \Upsilon_2^T \Upsilon_2.$$

Hence, $\Phi < 0$ if the following inequality holds:

$$\check{\Phi} + \frac{1}{\alpha_1} \Upsilon_1 \Upsilon_1^T + \alpha_1 \Upsilon_2^T \Upsilon_2 < 0.$$

Then, by premultiplying and postmultiplying $diag\{I, I, I, I, I, I, F_1^T\}$ and its transpose on both sides of $\check{\Phi}$, and using Lemma 3 again, it follows that

$$\bar{\Phi} = \begin{bmatrix} \bar{\Sigma}_{11} & \check{\Sigma}_{12} & \bar{\Sigma}_{13} & \Psi_1 & 0 & F_1^T \mathcal{B}_\tau & C^T \mathcal{K}^T F_1 & -F_1^T \mathcal{G} \\ * & -F_2^T - F_2 & -F_2^T \mathcal{K} & \Psi_2 & 0 & F_2^T \mathcal{B}_\tau & 0 & -F_2^T \mathcal{G} \\ * & * & \Sigma_{33} & 0 & 0 & 0 & \mathcal{K}^T F_1 & 0 \\ * & * & * & -2\Lambda_1 & 0 & 0 & 0 & 0 \\ * & * & * & * & \Psi_3 & L\Lambda_2 & 0 & 0 \\ * & * & * & * & * & -2\Lambda_2 & 0 & 0 \\ * & * & * & * & * & * & -F_1^T \mathcal{R}^{-1} F_1 & \mathcal{G} \\ * & * & * & * & * & * & * & -\alpha_1 I \end{bmatrix} < 0, \quad (3.33)$$

where

$$\bar{\Sigma}_{11} = F_1^T(-\mathcal{A} - \mathcal{K}C) + (-\mathcal{A} - \mathcal{K}C)^T F_1 + \epsilon C^T \Gamma C$$

$$\begin{aligned} & +2\gamma P + 2\gamma UL + S + Q + \alpha_1 C^T M^T M C, \\ \bar{\Sigma}_{13} & = -F_1^T \mathcal{K} + \alpha_1 C^T M^T M. \end{aligned}$$

For the item $-F_1^T \mathcal{R}^{-1} F_1$ of the matrix $\bar{\Phi}$, according to Lemma 2, the following inequality holds true:

$$\vartheta F_1 + \vartheta F_1^T \leq \vartheta^2 \mathcal{R} + F_1^T \mathcal{R}^{-1} F_1.$$

Note that

$$-F_1^T \mathcal{R}^{-1} F_1 \leq -\vartheta F_1 - \vartheta F_1^T + \vartheta^2 \mathcal{R},$$

so we can re-express (3.33) as (3.31) by setting

$$F_1^T \mathcal{K} = Y, F_2 = \kappa F_1.$$

Then, along similar lines as those for the above proof, (3.3) and (3.4) can be guaranteed by (3.29) and (3.30), respectively. The proof is completed. \square

Remark 5. Through the use of matrix congruence transformation and a few inequality techniques, a method for the design of the non-fragile controller is developed in Theorem 2. It is shown that the needed gain matrix can be obtained by solving multiple LMIs that can be readily verified by utilizing the MATLAB software.

When there is no gain perturbation, we can get the following corollary:

Corollary 1. For the given scalars $\kappa, \gamma > 0, \beta > 0, \epsilon \geq 0$, suppose that there exist $p \times p$ matrices $P > 0, N > 0, S > 0, W, W_1, F_1, E_1, E_2, E_3, Y, p \times p$ diagonal matrices $U > 0, \Lambda_1 > 0$ and $\Lambda_2 > 0$, and a $q \times q$ matrix $\Gamma \geq 0$ such that

$$F > 0, \tilde{\Theta}_0^* < 0, \tilde{\Theta}_1^* < 0, \tilde{\Phi}^* < 0, \quad (3.34)$$

where F is given in Theorem 1, and

$$\tilde{\Theta}_0^* = \begin{bmatrix} \Xi_{11} & \Xi_{12} & \Xi_{13} & \Psi_1 & 0 & F_1^T \mathcal{B}_\tau & 0 \\ * & \Xi_{22} & \Xi_{23} & \tilde{\Psi}_2 & 0 & \kappa F_1^T \mathcal{B}_\tau & 0 \\ * & * & \tilde{\Xi}_{33} & 0 & 0 & 0 & C^T Y^T \\ * & * & * & -2\Lambda_1 & 0 & 0 & 0 \\ * & * & * & * & \Psi_3 & L\Lambda_2 & 0 \\ * & * & * & * & * & -2\Lambda_2 & 0 \\ * & * & * & * & * & * & \Psi_4 \end{bmatrix},$$

$$\tilde{\Theta}_1^* = \begin{bmatrix} \Pi_{11} & \Pi_{12} & \Pi_{13} & \beta E_1^T & \Psi_1 & 0 & F_1^T \mathcal{B}_\tau & 0 \\ * & \Pi_{22} & \Pi_{23} & \beta E_2^T & \tilde{\Psi}_2 & 0 & \kappa F_1^T \mathcal{B}_\tau & 0 \\ * & * & \tilde{\Pi}_{33} & \beta E_3^T & 0 & 0 & 0 & C^T Y^T \\ * & * & * & -\beta e^{-2\gamma\beta} N & 0 & 0 & 0 & 0 \\ * & * & * & * & -2\Lambda_1 & 0 & 0 & 0 \\ * & * & * & * & * & \Psi_3 & L\Lambda_2 & 0 \\ * & * & * & * & * & * & -2\Lambda_2 & 0 \\ * & * & * & * & * & * & * & \Psi_4 \end{bmatrix},$$

$$\tilde{\Phi}^* = \begin{bmatrix} \tilde{\Sigma}_{11} & \Sigma_{12} & -Y & \Psi_1 & 0 & F_1^T \mathcal{B}_\tau & C^T Y^T \\ * & \Sigma_{22} & -\kappa Y & \tilde{\Psi}_2 & 0 & \kappa F_1^T \mathcal{B}_\tau & 0 \\ * & * & -\Gamma & 0 & 0 & 0 & Y^T \\ * & * & * & -2\Lambda_1 & 0 & 0 & 0 \\ * & * & * & * & \Psi_3 & L\Lambda_2 & 0 \\ * & * & * & * & * & -2\Lambda_2 & 0 \\ * & * & * & * & * & * & \Psi_4 \end{bmatrix},$$

with

$$\begin{aligned} \tilde{\Xi}_{33} &= E_3 + E_3^T - (1/2 - \gamma\beta)(W + W^T - 2W_1 - 2W_1^T), \\ \tilde{\Pi}_{33} &= E_3 + E_3^T - (1/2)(W + W^T - 2W_1 - 2W_1^T), \\ \tilde{\Sigma}_{11} &= -F_1^T \mathcal{A} - \mathcal{A}^T F_1 - YC - C^T Y^T + \epsilon C^T \Gamma C \\ &\quad + 2\gamma P + 2\gamma UL + S + Q, \end{aligned}$$

and the other notations are the same as those in Theorem 2. Then, the proposed controller (2.7) with the gain matrix

$$\mathcal{K} = (F_1^T)^{-1} Y$$

exponentially stabilizes the error system (2.10) under the conditions of the SETC mechanism, and the cost function in (2.11) satisfies $\mathcal{J}(\infty) \leq \varepsilon^T(0)(P + UL)\varepsilon(0) + \int_{-\tau}^0 \varepsilon^T(s)S\varepsilon(s)ds$.

3.3. Optimization scheme

Theorem 2 presents an approach to design the non-fragile cost-guaranteed controller and the event-trigger matrix. Based on Theorem 2, we can give an optimization scheme to estimate the minimum cost value of \mathcal{J}° . That is to say, the following theorem will present an approach to select a controller that can ensure the minimum upper bound of the guaranteed cost control performance index.

Before stating the Theorem 3, we define

$$\mathcal{H}\mathcal{H}^T = \int_{-\tau}^0 \varepsilon(s)\varepsilon^T(s)ds. \quad (3.35)$$

Theorem 3. Consider the error system (2.10) with the quadratic cost function in (2.11) if the optimization issue

$$\begin{aligned} \min \quad & \lambda_1 \varepsilon^T(0)\varepsilon(0) + \text{tr}(\Pi) \\ \text{subject to} \quad & (i) \text{ LMIs in (3.28),} \\ & (ii) P + UL < \lambda_1 I, \end{aligned} \quad (3.36)$$

$$(iii) \begin{bmatrix} -\Pi & \mathcal{H}^T \\ \mathcal{H} & -\mathcal{D} \end{bmatrix} < 0 \quad (3.37)$$

is solvable, where $\text{tr}(\Pi)$ denotes the trace of Π and $\mathcal{D} = S^{-1}$. Then the proposed control law $u(t)$ in (2.7) with the gain matrix (3.32) is an optimal event-triggered cost-guaranteed control law, and the quadratic cost function in (2.11) satisfies $\mathcal{J}(\infty) < \lambda_1 \varepsilon^T(0)\varepsilon(0) + \text{tr}(\Pi)$.

Proof. By (3.36), it is not difficult to see that there exists $\lambda_1 > 0$, such that

$$\varepsilon^T(0)(P + UL)\varepsilon(0) \leq \lambda_1 \varepsilon^T(0)\varepsilon(0).$$

In addition, from (3.35) and (3.37), we can write

$$\int_{-\tau}^0 \varepsilon^T(s)S\varepsilon(s)ds = \int_{-\tau}^0 \text{tr}(\varepsilon^T(s)S\varepsilon(s))ds = \text{tr}(\mathcal{H}\mathcal{H}^T S) = \text{tr}(\mathcal{H}^T \mathcal{D}^{-1}\mathcal{H}) < \text{tr}(\Pi).$$

Therefore, it follows from (3.27) that $\mathcal{J}(\infty) < \lambda_1 \varepsilon^T(0)\varepsilon(0) + \text{tr}(\Pi)$. Thus, the minimization of $\lambda_1 \varepsilon^T(0)\varepsilon(0) + \text{tr}(\Pi)$ implies the minimization of the cost-related performance index in Eq (3.27). The proof is complete. \square

When there is no gain perturbation, we can readily write the following result:

Corollary 2. Consider the error system (2.10) with the quadratic cost function in (2.11) if the optimization issue

$$\begin{aligned} \min \quad & \lambda_2 \varepsilon^T(0)\varepsilon(0) + \text{tr}(\Pi) \\ \text{subject to} \quad & (i) \text{ LMIs in (3.34),} \\ & (ii) P + UL < \lambda_2 I, \\ & (iii) \begin{bmatrix} -\Pi & \mathcal{H}^T \\ \mathcal{H} & -\mathcal{D} \end{bmatrix} < 0 \end{aligned}$$

is solvable, where $\text{tr}(\Pi)$ denotes the trace of Π and $\mathcal{D} = S^{-1}$. Then the proposed control law $u(t)$ in (2.7) with gain matrix (3.32) is an optimal event-triggered cost-guaranteed control law, and the quadratic cost function in (2.11) satisfies $\mathcal{J}(\infty) < \lambda_2 \varepsilon^T(0)\varepsilon(0) + \text{tr}(\Pi)$.

4. Numerical simulation

Consider TDNNs (2.1) and (2.3) with

$$\begin{aligned} \mathcal{A} &= \begin{bmatrix} 1 & 0 \\ 0 & 1 \end{bmatrix}, \quad \mathcal{B} = \begin{bmatrix} 2 & -0.1 \\ -5 & 3 \end{bmatrix}, \\ \mathcal{B}_\tau &= \begin{bmatrix} -1.5 & -0.1 \\ -0.2 & -2.5 \end{bmatrix}, \quad \mathcal{C} = \begin{bmatrix} 1 & -1 \\ 0 & 0.5 \end{bmatrix}. \end{aligned}$$

The activation function is chosen as $f(x(t)) = [\tanh(x_1(t)), \tanh(x_2(t))]^T$. Note that $f(x(t))$ satisfies Assumption 1 with $L = \text{diag}\{1, 1\}$. And the time delay is taken as $\tau(t) = 1 + 0.2 \sin(2t)$, which implies $\mu = 0.4$ and $\tau = 1.2$.

In the simulation, the initial conditions of the drive and response systems were set to be $x(s) = [-0.27 \ -0.24]^T$ and $\hat{x}(s) = [0.42 \ -0.24]^T$, respectively, where $s \in [-\tau, 0]$. The chaotic attractor of the drive TDNN is depicted in Figure 1. Simultaneously, from (3.35), we have

$$\mathcal{H} = \begin{bmatrix} 0.76 & 0 \\ 0 & 0 \end{bmatrix}.$$

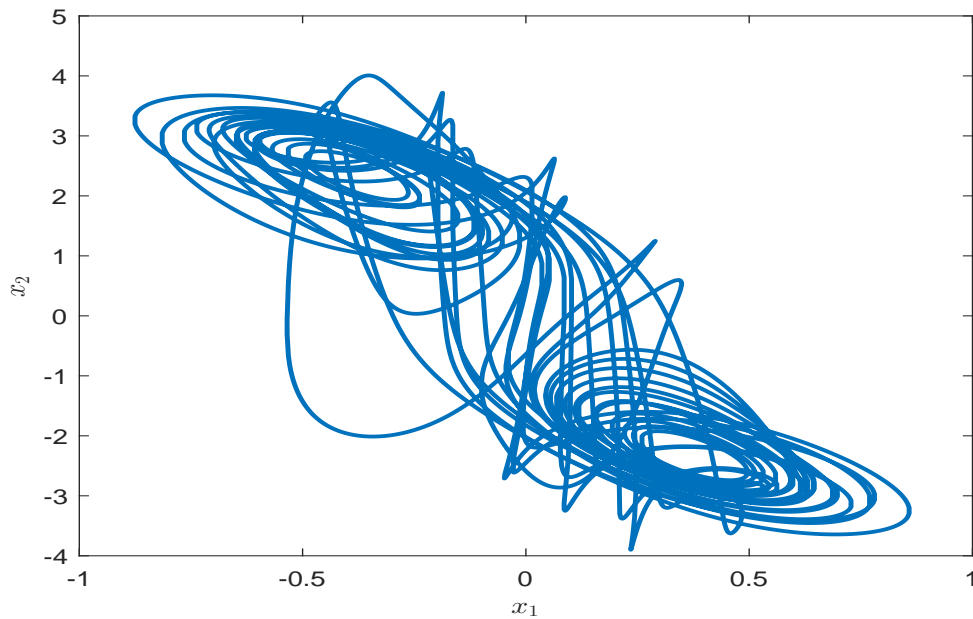


Figure 1. Chaotic behaviors of the drive TDNN.

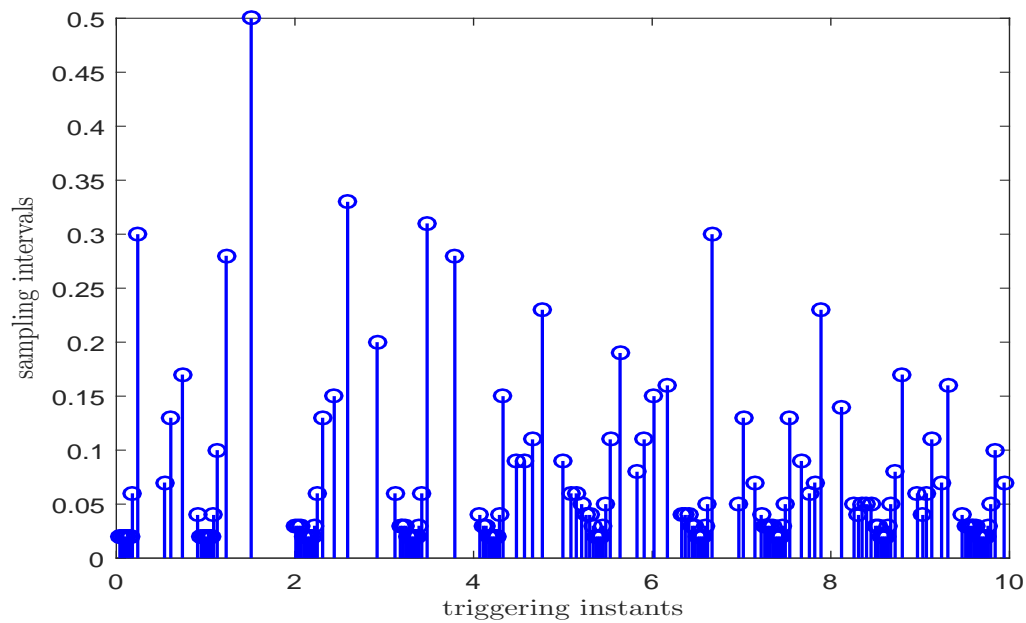


Figure 2. Triggering moments and sampling intervals.

The two parameter matrices in the quadratic cost function (2.11) were chosen as

$$Q = \begin{bmatrix} 1 & 0 \\ 0 & 1 \end{bmatrix}, \mathcal{R} = \begin{bmatrix} 0.1 & 0 \\ 0 & 0.1 \end{bmatrix}.$$

Given $\beta = 0.02$ and $\epsilon = 0.2$, the following SETC mechanism can be obtained:

$$\alpha_{k+1} = \min \left\{ t \geq \alpha_k + 0.02 \mid (\bar{y}(t) - \bar{y}(\alpha_k))^T \Gamma (\bar{y}(t) - \bar{y}(\alpha_k)) \geq 0.2 \bar{y}^T(t) \Gamma \bar{y}(t) \right\}.$$

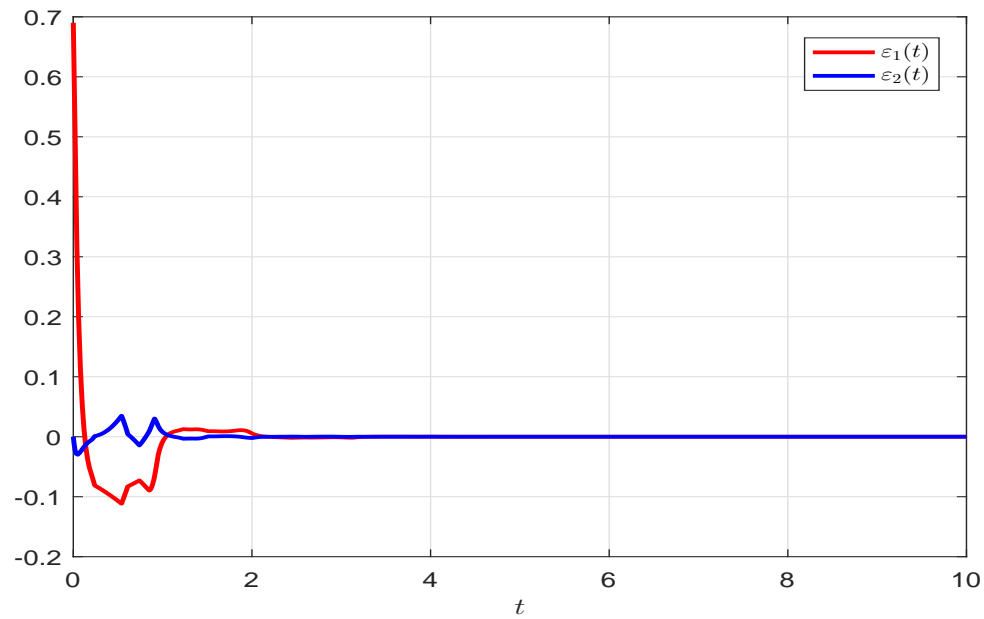


Figure 3. State response of the error system.

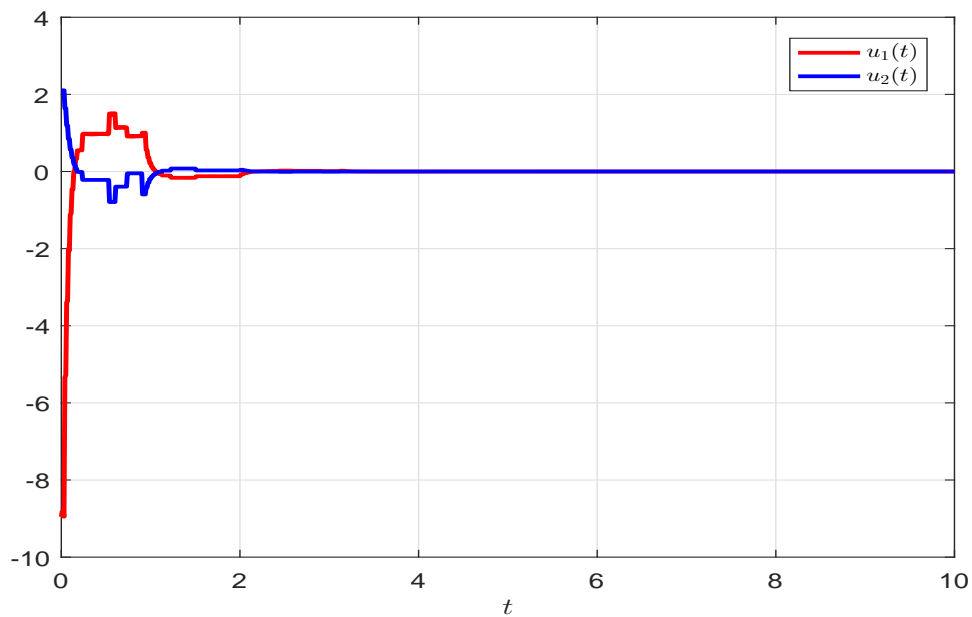


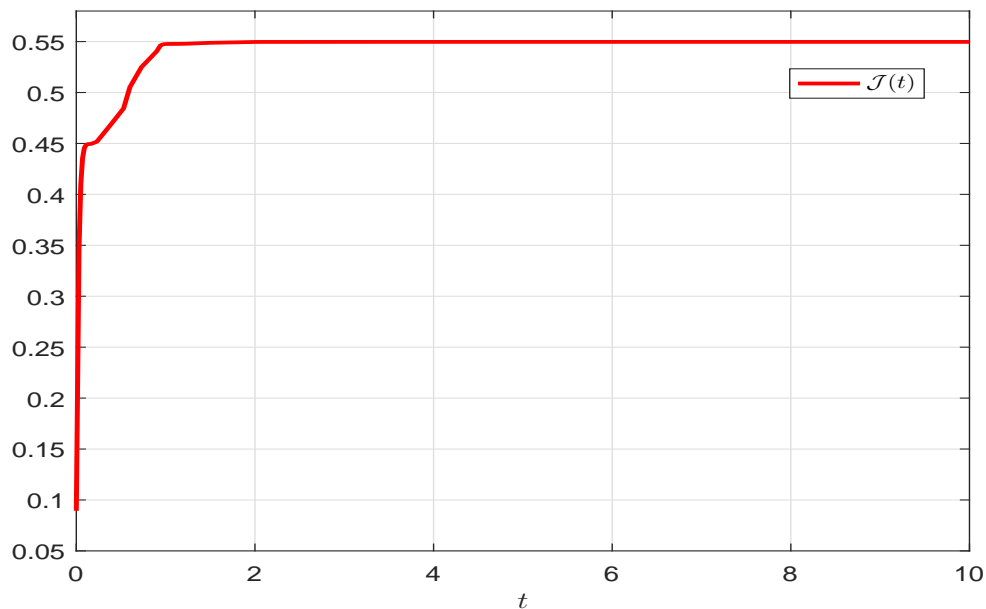
Figure 4. Control input signals.

Next, let us show the applicability of the present non-fragile control approaches. The parameter matrices for the gain perturbation $\Delta\mathcal{K}$ in (2.4) were set to be

$$\mathcal{G} = g \begin{bmatrix} 0.5 & 0 \\ 0 & 0.5 \end{bmatrix}, \mathcal{M} = \begin{bmatrix} 1 & 0 \\ 0 & 1 \end{bmatrix}, \mathcal{T}(t) = 0.8 |\sin(t)|.$$

Table 1. Optimal cost-related performance \mathcal{J}° for different values of g .

Conditions	Theorem 3			Corollary 2
g	0.5	0.3	0.1	0
\mathcal{K}	$\begin{bmatrix} 12.0928 & 20.3418 \\ -2.9653 & 20.7362 \end{bmatrix}$	$\begin{bmatrix} 11.9176 & 20.1074 \\ -2.9347 & 20.5661 \end{bmatrix}$	$\begin{bmatrix} 11.7517 & 19.8843 \\ -2.9067 & 20.3973 \end{bmatrix}$	$\begin{bmatrix} 11.6721 & 19.7769 \\ -2.8936 & 20.3135 \end{bmatrix}$
Γ	$\begin{bmatrix} 48.1832 & 49.9208 \\ 49.9208 & 224.3081 \end{bmatrix}$	$\begin{bmatrix} 45.4914 & 47.5788 \\ 47.5788 & 216.3803 \end{bmatrix}$	$\begin{bmatrix} 43.0504 & 45.4469 \\ 45.4469 & 208.9249 \end{bmatrix}$	$\begin{bmatrix} 41.9143 & 44.4511 \\ 44.4511 & 205.3583 \end{bmatrix}$
\mathcal{J}°	1.7812	1.6990	1.6237	1.5883

**Figure 5.** $\mathcal{J}(t)$ along the system (2.10).

We choose $\gamma = 0.01$, $\vartheta = 19.2$, and $\kappa = 0.1$. Then, for different values of the parameter g , by using Theorem 3 and Corollary 2, the controller gain \mathcal{K} , triggered matrix Γ , and optimal cost-related performance index \mathcal{J}° were obtained as shown Table 1. From the table we can find that \mathcal{J}° will increase as g increases. Based on the above parameters, by utilizing MATLAB, the triggered moments and the corresponding sampled intervals were obtained as shown in Figure 2. The trajectories of the error system (2.10) and input signals are shown in Figures 3 and 4, respectively. Obviously, the trajectories of the state and input quickly converged to 0. Figure 5 shows the trajectory of $\mathcal{J}(t)$. It was found that $\mathcal{J}(t)$ converged to 0.5497 (i.e., $\mathcal{J}(\infty) = 0.5497$), which is less than $\mathcal{J}^\circ = 1.6237$. Thus, the simulations verify the present theoretical results.

5. Conclusions

The non-fragile event-triggered CGSC of TDNNs has been investigated. From the point of view of saving computational and network resources, a SETC mechanism has been introduced to determine the event-triggering moments. A piecewise functional $\mathcal{V}(t)$ has been constructed to make efficient use of the sampling intervals $[\alpha_k, \alpha_{k+1})$ and activation function $\bar{f}(\varepsilon(t))$. With the help of the constructed functional and several inequalities, a criterion (see Theorem 1) has been derived to ensure the exponential stability and the cost-related performance of the synchronization-error system. Based on the criterion, a novel joint design of the designed control gain and trigger matrix has been developed (i.e., Theorem 2), and an optimization scheme for the minimum cost-related performance index has been given (i.e., Theorem 3). The validity and practicability of the obtained results have been illustrated through a numerical example. Future research will be focused on the event-triggered synchronization control of TDNNs under cyber attack.

Acknowledgments

This work was supported by the Key Research and Development Project of Anhui Province (Grant No. 202004a07020028).

Conflict of interest

The authors declare that there is no conflict of interest.

References

1. W. Ren, R. W. Beard, Speech synthesis from neural decoding of spoken sentences, *Nature*, **568** (2019), 493–498. <https://doi.org/10.1038/s41586-019-1119-1>
2. F. A. Gers, E. Schmidhuber, LSTM recurrent networks learn simple context-free and context-sensitive languages, *IEEE Trans. Neural Netw.*, **12** (2001), 1333–1340. <https://doi.org/10.1109/72.963769>
3. R. K. Brouwer, Growing of a fuzzy recurrent artificial neural network (FRANN) for pattern classification, *Int. J. Neural Syst.*, **9** (1999), 335–350. <https://doi.org/10.1142/S0129065799000320>
4. H. Hewamalage, C. Bergmeir, K. Bandara, Recurrent neural networks for time series forecasting: Current status and future directions, *Int. J. Forecasting*, **37** (2021), 388–427. <https://doi.org/10.1016/j.ijforecast.2020.06.008>
5. Y. Cao, R. Sriraman, N. Shyamsundarraaj, R. Samidurai, Robust stability of uncertain stochastic complex-valued neural networks with additive time-varying delays, *Math. Comput. Simul.*, **171** (2020), 207–220. <https://doi.org/10.1016/j.matcom.2019.05.011>
6. T. H. Lee, H. M. Trinh, J. H. Park, Stability analysis of neural networks with time-varying delay

- by constructing novel Lyapunov functionals, *IEEE Trans. Neural Netw. Learn. Syst.*, **29** (2018), 4238–4247. <https://doi.org/10.1109/TNNLS.2017.2760979>
7. S. Arik, New criteria for stability of neutral-type neural networks with multiple time delays, *IEEE Trans. Neural Netw. Learn. Syst.*, **31** (2020), 1504–1513. <https://doi.org/10.1109/TNNLS.2019.2920672>
 8. N. M. Thoiyab, P. Muruganatham, Q. Zhu, N. Gunasekaran, Novel results on global stability analysis for multiple time-delayed BAM neural networks under parameter uncertainties, *Chaos Solitons Fractals*, **152** (2021), 111441. <https://doi.org/10.1016/j.chaos.2021.111441>
 9. L. Fan, Q. Zhu, Mean square exponential stability of discrete-time Markov switched stochastic neural networks with partially unstable subsystems and mixed delays, *Inf. Sci.*, **580** (2021), 243–259. <https://doi.org/10.1016/j.ins.2021.08.068>
 10. Q. Wu, Z. Yao, Z. Yin, H. Zhang, Fin-TS and Fix-TS on fractional quaternion delayed neural networks with uncertainty via establishing a new Caputo derivative inequality approach, *Math. Biosci. Eng.*, **19** (2022), 9220–9243. <https://doi.org/10.3934/mbe.2022428>
 11. W. Tai, D. Zuo, Z. Xuan, J. Zhou, Z. Wang, Non-fragile $L_2 - L_\infty$ filtering for a class of switched neural networks, *Math. Comput. Simul.*, **185** (2021), 629–645. <https://doi.org/10.1016/j.matcom.2021.01.014>
 12. J. Cheng, L. Liang, H. Yan, J. Cao, S. Tang, K. Shi, Proportional-integral observer-based state estimation for Markov memristive neural networks with sensor saturations, *IEEE Trans. Neural Netw. Learn. Syst.*, 2022. <https://doi.org/10.1109/TNNLS.2022.3174880>
 13. N. Gunasekaran, M. S. Ali, Design of stochastic passivity and passification for delayed BAM neural networks with Markov jump parameters via non-uniform sampled-data control, *Neural Process. Lett.*, **53** (2021), 391–404. <https://doi.org/10.1007/s11063-020-10394-6>
 14. A. Abdurahman, H. Jiang, C. Hu, Z. Teng, Parameter identification based on finite-time synchronization for Cohen–Grossberg neural networks with time-varying delays, *Nonlinear Anal., Model. Control*, **20** (2015), 348–366. <https://doi.org/10.15388/NA.2015.3.3>
 15. M. Kalpana, K. Ratnavelu, P. Balasubramaniam, M. Z. M. Kamali, Synchronization of chaotic-type delayed neural networks and its application, *Nonlinear Dyn.*, **93** (2018), 543–555. <https://doi.org/10.1007/s11071-018-4208-z>
 16. A. M. Alimi, C. Aouiti, E. A. Assali, M. Z. M. Kamali, Finite-time and fixed-time synchronization of a class of inertial neural networks with multi-proportional delays and its application to secure communication, *Neurocomputing*, **332** (2019), 29–43. <https://doi.org/10.1016/j.neucom.2018.11.020>
 17. T. H. Lee, J. H. Park, Improved criteria for sampled-data synchronization of chaotic Lur’e systems using two new approaches, *Nonlin. Anal. Hybrid Syst.*, **24** (2017), 132–145. <https://doi.org/10.1016/j.nahs.2016.11.006>

18. L. Wang, Y. Shen, G. Zhang, Synchronization of a class of switched neural networks with time-varying delays via nonlinear feedback control, *IEEE Trans. Cybern.*, **46** (2016), 2300–2310. <https://doi.org/10.1109/TCYB.2015.2475277>
19. Y. Zhao, X. Li, P. Duan, Observer-based sliding mode control for synchronization of delayed chaotic neural networks with unknown disturbance, *Neural Networks*, **117** (2019), 268–273. <https://doi.org/10.1016/j.neunet.2019.05.013>
20. D. Tong, L. Zhang, W. Zhou, J. Zhou, Y. Xu, Asymptotical synchronization for delayed stochastic neural networks with uncertainty via adaptive control, *Int. J. Control Autom. Syst.*, **14** (2016), 706–712. <https://doi.org/10.1007/s12555-015-0077-0>
21. H. Li, C. Li, D. Ouyang, S. K. Nguang, Impulsive synchronization of unbounded delayed inertial neural networks with actuator saturation and sampled-data control and its application to image encryption, *IEEE Trans. Neural Networks Learn. Syst.*, **32** (2021), 1460–1473. <https://doi.org/10.1109/TNNLS.2020.2984770>
22. G. Chen, J. Xia, J. H. Park, H. Shen, G. Zhuang, Sampled-data synchronization of stochastic Markovian jump neural networks with time-varying delay, *IEEE Trans. Neural Networks Learn. Syst.*, **33** (2022), 3829–3841. <https://doi.org/10.1109/TNNLS.2021.3054615>
23. M. Dlala and S. O. Alrashidi, Rapid exponential stabilization of Lotka-McKendrick’s equation via event-triggered impulsive control, *Math. Biosci. Eng.*, **18** (2021), 9121–9131. <https://doi.org/10.3934/mbe.2021449>
24. Z. Gu, S. Yan, J. H. Park, X. Xie, Event-triggered synchronization of chaotic Lur’e systems via memory-based triggering approach, *IEEE Trans. Circuits Syst. II Express Briefs*, **69** (2022), 1427–1431. <https://doi.org/10.1109/TCSII.2021.3113955>
25. J. Wu, S. Qiu, M. Liu, H. Li, Y. Liu, Finite-time velocity-free relative position coordinated control of spacecraft formation with dynamic event triggered transmission, *Math. Biosci. Eng.*, **19** (2022), 6883–6906. <https://doi.org/10.3934/mbe.2022324>
26. J. Cheng, J. H. Park, Z. Wu, Observer-based asynchronous control of nonlinear systems with dynamic event-based try-once-discard protocol, *IEEE Trans. Cybern.*, 2021. <https://doi.org/10.1109/TCYB.2021.3104806>
27. J. Lunze, D. Lehmann, A state-feedback approach to event-based control, *Automatica*, **46** (2010), 211–215. <https://doi.org/10.1016/j.automatica.2009.10.035>
28. D. Yue, E. Tian, Q. Han, A delay system method for designing event-triggered controllers of networked control systems, *IEEE Trans. Autom. Control*, **58** (2012), 475–481. <https://doi.org/10.1109/TAC.2012.2206694>
29. M. Xing, F. Deng, X. Zhao, Synchronization of stochastic complex dynamical networks under self-triggered control, *Int. J. Robust Nonlinear Control*, **27** (2017), 2861–2878. <https://doi.org/10.1002/rnc.3716>

30. J. Zhang, E. Fridman, Dynamic event-triggered control of networked stochastic systems with scheduling protocols, *IEEE Trans. Autom. Control*, **66** (2021), 6139–6147. <https://doi.org/10.1109/TAC.2021.3061668>
31. A. Selivanov, E. Fridman, Event-triggered H_∞ control: A switching approach, *IEEE Trans. Autom. Control*, **61** (2015), 3221–3226. <https://doi.org/10.1109/TAC.2015.2508286>
32. Z. Yan, X. Huang, J. Cao, Variable-sampling-period dependent global stabilization of delayed memristive neural networks based on refined switching event-triggered control, *Sci. China Inf. Sci.*, **63** (2020), 212201. <https://doi.org/10.1007/s11432-019-2664-7>
33. S. Ding, X. Xie, Y. Liu, Event-triggered static/dynamic feedback control for discrete-time linear systems, *Inf. Sci.*, **524** (2020), 33–45. <https://doi.org/10.1016/j.ins.2020.03.044>
34. W. Wu, L. He, J. Zhou, Z. Xuan, S. Arik, Disturbance-term-based switching event-triggered synchronization control of chaotic Lurie systems subject to a joint performance guarantee, *Commun. Nonlinear Sci. Numer. Simul.*, **115** (2022), 106774. <https://doi.org/10.1016/j.cnsns.2022.106774>
35. W. Wang, D. Xu, J. Zhou, Z. Yan, Cost-guaranteed exponential stabilization of Lurie systems via switched event-triggered control, *Discrete Cont. Dyn. B*, 2022. <https://doi.org/10.3934/dcdsb.2022194>
36. Y. Zhou, H. Zhang, Z. Zeng, Quasisynchronization of memristive neural networks with communication delays via event-triggered impulsive control, *IEEE Trans. Cybern.*, **52** (2022), 7682–7693. <https://doi.org/10.1109/TCYB.2020.3035358>
37. Z. Yan, X. Huang, Y. Fan, J. Xia, H. Shen, Threshold-function-dependent quasi-synchronization of delayed memristive neural networks via hybrid event-triggered control, *IEEE Trans. Syst., Man, Cybern.*, **51** (2021), 6712–6722. <https://doi.org/10.1109/TSMC.2020.2964605>
38. S. Yan, S. K. Nguang, Z. Gu, H_∞ weighted integral event-triggered synchronization of neural networks with mixed delays, *IEEE Trans. Ind. Informat.*, **17** (2021), 2365–2375. <https://doi.org/10.1109/TII.2020.3004461>
39. X. Chang, Y. Liu, M. Shen, Resilient control design for lateral motion regulation of intelligent vehicle, *IEEE ASME Trans. Mechatronics*, **24** (2019), 2488–2497. <https://doi.org/10.1109/TMECH.2019.2946895>
40. J. Zhou, Y. Liu, J. Xia, Z. Wang, S. Arik, Resilient fault-tolerant anti-synchronization for stochastic delayed reaction–diffusion neural networks with semi-Markov jump parameters, *Neural Networks*, **125** (2020), 194–204. <https://doi.org/10.1016/j.neunet.2020.02.015>
41. R. Sakthivel, C. Wang, S. Santra, B. Kaviarasan, Non-fragile reliable sampled-data controller for nonlinear switched time-varying systems, *Nonlin. Anal. Hybrid Syst.*, **27** (2018), 62–76. <https://doi.org/10.1016/j.nahs.2017.08.005>
42. J. H. Park, H. Shen, X. Chang, T. H. Lee, Fuzzy resilient energy-to-peak filter design for continuous-time nonlinear systems, in *Recent Advances in Control and Filtering*

- of *Dynamic Systems with Constrained Signals*, Cham: Springer, (2019), 119–139. <https://doi.org/10.1007/978-3-319-96202-3>
43. X. Chang, *Takagi-Sugeno Fuzzy Systems Non-fragile H-infinity Filtering*, Berlin: Springer-Verlag, 2012. <https://doi.org/10.1007/978-3-642-28632-2>
 44. L. Chen, Y. Chen, N. Zhang, Synchronization control for chaotic neural networks with mixed delays under input saturations, *Neural Process. Lett.*, **53** (2021), 3735–3755. <https://doi.org/10.1007/s11063-021-10577-9>
 45. L. He, W. Wu, Q. Zhu, G. Yao, J. Zhou, Input-to-state stabilization of delayed semi-Markovian jump neural networks via sampled-data control, *Neural Process. Lett.*, 2022. <https://doi.org/10.1007/s11063-022-11008-z>
 46. H. Lu, Chaotic attractors in delayed neural networks, *Phys. Lett. A*, **298** (2002), 109–116. [https://doi.org/10.1016/S0375-9601\(02\)00538-8](https://doi.org/10.1016/S0375-9601(02)00538-8)
 47. S. Santra, R. Sakthivel, K. Mathiyalagan, A. S. Marshal, Exponential passivity results for singular networked cascade control systems via sampled-data control, *J. Dyn. Syst., Means. Control*, **139** (2017). <https://doi.org/10.1115/1.4034781>
 48. M. S. Ali, N. Gunasekaran, J. Cao, Sampled-data state estimation for neural networks with additive time-varying delays, *Acta Math. Sci.*, **39** (2019), 195–213. <https://doi.org/10.1007/s10473-019-0116-7>
 49. N. Gunasekaran, G. Zhai, Q. Yu, Sampled-data synchronization of delayed multi-agent networks and its application to coupled circuit, *Neurocomputing*, **413** (2020), 499–511. <https://doi.org/10.1016/j.neucom.2020.05.060>
 50. S. Santra, M. Joby, M. Sathishkumar, S. M. Anthoni, LMI approach-based sampled-data control for uncertain systems with actuator saturation: application to multi-machine power system, *Nonlinear Dyn.*, **107** (2022), 967–982. <https://doi.org/10.1007/s11071-021-06995-y>
 51. N. Gunasekaran, M. S. Ali, S. Arik, H. A. Ghaffar, A. A. Z. Diab, Finite-time and sampled-data synchronization of complex dynamical networks subject to average dwell-time switching signal, *Neural Networks*, **149** (2022), 137–145. <https://doi.org/10.1016/j.neunet.2022.02.013>
 52. K. Gu, J. Chen, V. L. Kharitonov, *Stability of Time-Delay Systems*, Boston, MA: Birkhauser, 2003. <https://doi.org/10.1007/978-1-4612-0039-0>
 53. K. Zhou and P. P. Khargonekar, Robust stabilization of linear systems with norm-bounded time-varying uncertainty, *Syst. Contr. Lett.*, **10** (1988), 17–20. [https://doi.org/10.1016/0167-6911\(88\)90034-5](https://doi.org/10.1016/0167-6911(88)90034-5)
 54. S. Boyd, L. E. Ghaoui, E. Feron, V. Balakrishnan, *Linear Matrix Inequalities in System and Control Theory*, Philadelphia, PA: SIAM, 1994. <https://doi.org/10.1137/1.9781611970777>



AIMS Press

©2023 the Author(s), licensee AIMS Press. This is an open access article distributed under the terms of the Creative Commons Attribution License (<http://creativecommons.org/licenses/by/4.0>)